A More Expressive 3D Region Connection Calculus

Chaman Sabharwal
Missouri University of Science and Technology

A More Expressive 3D Region Connection Calculus

Chaman L. Sabharwal, Jennifer L. Leopold, Nathan Eloe

Department of Computer Science
Missouri University of Science and Technology
Rolla, MO - 65409, USA
chaman@mst.edu, leopoldj@mst.edu, nwe5q8@mst.edu

Abstract Spatial qualitative analysis in 3D provides engineers with the ability to visually evaluate interference between parts, complicated geometric features, required tolerances, mechanism motion, and various aspects of assembly structure. Yet, despite the fact that 3D technology has been well developed for several years, many mechanical engineering designers currently do not use 3D CAD technology, and research in qualitative spatial reasoning continues to focus on 2D perspectives of 3D objects. In part, this is due to human cognitive limitations and the increased computational complexity of 3D modeling. However, given the greater wealth of information that can be obtained when additional dimensions are considered, and the enormous amount of 3D image data that are available, research efforts in this area should continue. Herein we present an extension of our previous work to combine quantitative and qualitative reasoning in 3D. The enhanced model is more expressive in that it now distinguishes several types of obscuration. Further, it differs from other region connection calculi used for qualitative spatial reasoning in that it determines the composite (topological plus obscuration) relation between two objects in 3D, not 2D.

Keywords-qualitative spatial reasoning; region connection calculus; 3D

I. INTRODUCTION

Computational spatial reasoning is useful for many applications, such as geographic information systems, image processing, and robotics. As with any knowledge representation and reasoning system, having additional dimensions of information often facilitates more accurate and informative analyses. Yet research in and implementations of qualitative spatial reasoning mostly have been limited to 2D, even when higher dimensions of data are available. In part, this is due to human cognitive limitations and the increased computational complexity that results when additional information is considered. However, given the enormous amount of 3D image data that continue to become available, as well as the increasing sophistication of mechanical and software systems that require spatial awareness, it is important that efforts to produce 3D spatial reasoning systems continue.

Herein we present an extension of our previous efforts to combine quantitative and qualitative reasoning in 3D [1]. This new model increases the expressive power by considering additional types of obscuration. Further, it differs from other region connection calculi in that it determines the composite (topological plus obscuration) relation between a pair of objects in 3D, not just 2D.

II. RELATED WORK

A. *Region Connection Calculi*

Much of the foundational research on qualitative spatial reasoning is based on a region connection calculus that describes 2D regions by their possible relations to each other. Most notable are the RCC-5 and RCC-8 models [2, 3]. The RCC-5 relations are: *disconnected* (DC), *partial overlap* (PO), *equal* (EQ), *proper part* (PP), and *proper part inverse* (PPi). RCC-8 differs from RCC-5 in that it adds a relation for *externally connected* (EC), distinguishes PP as two relations, *tangential proper part* (TPP) and *non-tangential proper part* (NTPP), and separates the inverse relation PPi into TPPi and NTPPi.

RCC-23 [4] extends RCC-8 to 23 relations in order to accommodate concave regions in 2D. This expanded set of relations is based on primitives for connection and convex hull (i.e., primitives for *inside*, *partially inside*, *outside*, and an inverse for each of those three relations). In addition to the PO, EQ, TPP, TPPi, NTPP, and NTPPi, relations of RCC-8, RCC-23 distinguishes eight relations for DC (based on the aforementioned convexity predicates), and nine relations for EC (also based on the convexity predicates).

RCC-62 [5] is even more expressive than RCC-23; whereas RCC-23 considers a concave region as one whole part, RCC-62 decomposes such a region into an outside, boundary, interior, and inside. The resulting 62 relations are based on a 16-Intersection that compares one object's outside, boundary, interior, and inside with those of another object. However, like RCC-8 and RCC-23, RCC-62 only describes the relationship between regions considering two dimensions.

In contrast to RCC-8, RCC-23, and RCC-62, the LOS-14 [6] and ROC-20 [7] models qualify the spatial relation between 2D regions in terms of the obscuration that occurs between them. LOS-14 differs from ROC-20 in that it is restricted to objects that do not overlap in 3D. The 14 relations of LOS-14 describe the spatial relationship between two 2D objects in terms of whether or not one completely or partially hides the other using a qualitative depth relation between the objects; one object can be in front of another, but the two cannot be of equal depth. ROC-20 extends LOS-14 by allowing objects to be concave (and hence accommodates mutual occlusion, adding 6 relations to the LOS-14 set). ROC-20 defines all spatial relations in terms of a combination of occlusion (i.e., *NonOccludes*, *PartiallyOccludes*, *MutuallyOccludes,* and *TotallyOccludes*) and, as applicable, an RCC-8 relation.

B. RCC-3D

In the aforementioned RCC-based models, the complete spatial relationship, not just the degree of obscuration, is only with respect to a particular 2D viewpoint. Over the past two years, the authors have investigated a different approach for spatially reasoning over 3D objects. An extensive discussion of that early model (named RCC-3D) is beyond the scope of this paper; see [1] for those details. Briefly, RCC-3D defines 13 spatial relations based on an 8-Intersection of the 3D interior, exterior, and boundary of the two objects, and a 3-Intersection of the 2D interior and exterior of a particular projection of the two objects in the view reference plane. Employing a naming convention similar to that used for RCC-8, although using *c* to represent *converse* rather than *i* for *inverse*, the 13 RCC-3D relations are: DC, DC_pp, DC_p, EC, EC_Pp, EC_P, PO_Pp, PO_P, TPP_P, TPP_Pc, EQ_P, $NTPP_P$, and $NTPP_P$c; the subscript *P* in the relation name represents the particular 2D projection plane, and partial obscuration (as opposed to complete obscuration) is indicated by adding a (non-subscripted) *p* to the end of the relation name.

As has been done for other region connection calculi, a conceptual neighborhood graph (CNG) was defined for RCC-3D to identify those transitions that can occur when the geometry of one object in a pair is changed gradually. For RCC-3D the topological distance between relations is computed as the number of intersections that change from empty to not empty (or vice versa), from one relation to another. This distance is expressed using the format x+y where x is computed by considering the 8-Intersection in 3D (hence, the inter-relation distance), and y is calculated based on the 3-Intersection in 2D projection plane P (the intra-relation distance).

A Prolog program was written to generate a composition table (CT) for RCC-3D, providing the ability to answer questions such as, "given three objects, A, B, and C, and knowledge of relations R_1(A, B), and R_2(B, C), what can be said about the relation between A and C." A prototype RCC-3D reasoner was then implemented, and tested to compare automated determination of spatial relationships between 3D reconstructions of anatomy (in OBJ file format) against the determination of experts who had examined the original specimens manually. The preliminary results [1] were very promising, and work commenced to create an application that would allow the user to check for inconsistency in relations between abstract temporal "states" of the objects, and determine possible relations that would have had to occur to transition from one state to another; the integration of that functionality together with a visual user interface was named VRCC-3D [8].

III. VRCC-3D+

Although the early RCC-3D and VRCC-3D models showed potential for studies involving spatial data, the authors realized that ambiguous analyses could occur in certain situations. As shown in Fig. 1, it is not possible to determine intersection or obscuration in 3D from only the 2D projections; that is, we cannot say that, just because the projections intersect, the objects intersect in 3D space. More precisely, in VRCC-3D, if we know R_1(A, B), R_2(B, C), Obs_1(A, B, P), and Obs_2(B, C, P) (where R_i is one of the spatial relations and Obs_i is one of the obscuration relations), then we can only determine R_3(A, C) and Obs_3(A, C, P); we cannot tell whether A is in front of C, or C is in front of A. In projections, the information about the distance from the projection plane is lost.

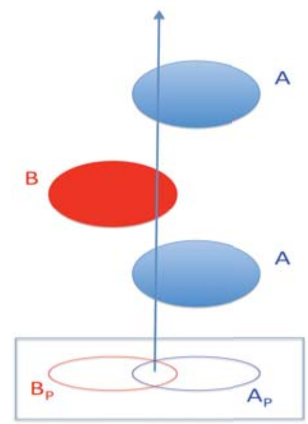

Figure 1. Shown are two configurations of object A relative to object B. From the intersection of projections A_P and B_P (where P is a 2D projection plane), it is not possible to determine: (1) if A and B intersect in 3D space, and (2) if A is in front of B, or B is in front of A.

To address this problem, the enhanced model described herein, VRCC-3D+, uses a depth parameter to distinguish additional types of obscuration. The result is a more expressive region connection calculus; the number of obscuration relations increases from 2 to 11, and the number of composite relations increases from 13 to 34 from VRCC-3D to VRCC-3D+, respectively.

A. Characterization of Base Relations

As with our earlier models, the eight base relations of VRCC-3D+ (which comprise the entire set of relations for RCC-8) are distinguished based on an 8-Intersection; see Table I. This is similar to the 9-Intersection presented in [9], with two notable exceptions: (1) the intersection between the exterior of one object and the exterior of another object is excluded since it will be non-empty for any pair of bounded objects (i.e., the intersection of the exteriors of two objects is not informative), and (2) the intersection predicates are computed for the 3D (not 2D) interior, boundary, and exterior of the objects.

	IntInt	IntBnd	IntExt	BndInt	BndBnd	BndExt	ExtInt	ExtBnd
DC	∅	∅	¬∅	∅	∅	¬∅	¬∅	¬∅
EC	∅	∅	¬∅	∅	¬∅	¬∅	¬∅	¬∅
EQ	¬∅	∅	∅	∅	¬∅	∅	∅	∅
NTPP	¬∅	∅	∅	¬∅	∅	∅	¬∅	¬∅
NTPPc	¬∅	¬∅	¬∅	∅	∅	¬∅	∅	∅
PO	¬∅	¬∅	¬∅	¬∅	¬∅	¬∅	¬∅	¬∅
TPP	¬∅	∅	∅	¬∅	¬∅	∅	¬∅	¬∅
TPPc	¬∅	¬∅	¬∅	∅	¬∅	¬∅	∅	∅

TABLE I. 8-Intersection Characterization Table (Int = Interior, Bnd = Boundary, Ext = Exterior; ¬∅= non-empty intersection, ∅ = empty intersection)

B. *Characterization of Obscuration*

Like ROC-20, VRCC-3D+ distinguishes non-occlusion, partial occlusion, and complete occlusion. However, for the VRCC-3D+ model it is assumed that all objects are opaque, so the ROC-20 notion of mutual occlusion (e.g., A obscures B, and B obscures A from a particular view reference point) is not supported. Instead VRCC-3D+ defines an equal occlusion, whereby the qualitative distance between two objects is represented with a predicate, *InFront,* that is computed with respect to a particular 3D viewpoint. Hence, the obscuration part of a VRCC-3D+ relation is determined by examining the three intersections between the 2D interior and exterior of each object (as had been done for the earlier model, VRCC-3D). But now an additional fourth parameter is incorporated into those definitions to represent the relative qualitative depths of the objects.

The names of the VRCC-3D+ obscuration types are of the form *xObsy*, where *Obs* refers to the intersection between the projections. Possible values for the prefix *x* are: *n* (no occlusion), *p* (partial occlusion), *e* (equal occlusion), and *c* (complete occlusion). The suffix *y* in the relation name refers to the value of *InFront*. When comparing two objects A and B, the suffix is blank when A is in front of B; a suffix of *_e* indicates that the two objects are equidistant from the view plane; the suffix *_c* indicates that B is closer to the view plane than A. There are a total of eleven occlusion relations, which are characterized in Table II. It should be noted that the particular 2D projection plane is not specified for each obscuration type listed in Table II because the results would be the same regardless of the reference plane; this will be the case for all tables that subsequently appear herein.

Not every type of obscuration is applicable to every base relation in VRCC-3D+. For example, it is not possible to have two objects, A and B, where A partially overlaps B in 3D space, but the projection of A does not overlap the projection of B for any viewpoint. All the possible combinations comprise a set of 34 relations for VRCC-3D+, as shown in Table III.

	IntInt	IntExt	ExtInt	InFront
pObs	¬∅	{∅,¬∅}	¬∅	Y
pObs_c	¬∅	¬∅	{∅,¬∅}	N
pObs_e	¬∅	¬∅	¬∅	E
cObs	¬∅	¬∅	∅	Y
cObs_c	¬∅	∅	¬∅	N
eObs_e	¬∅	∅	∅	E
eObs_c	¬∅	∅	∅	N
eObs	¬∅	∅	∅	Y
nObs_e	∅	¬∅	¬∅	E
nObs_c	∅	¬∅	¬∅	N
nObs	∅	¬∅	¬∅	Y

TABLE II. 3-Intersection + Depth Characterization Table (Int = Interior, Ext = Exterior; ¬∅= non-empty intersection, ∅ = empty intersection; Y = yes, N = no, E = equal)

	nObs	nObs_c	nObs_e	pObs	pObs_c	pObs_e	eObs	eObs_c	eObs_e	cObs	cObs_c
DC	X	X	X	X	X		X	X		X	X
EC	X	X	X	X	X		X	X		X	X
PO				X	X	X	X	X		X	X
EQ									X		
TPP								X	X		X
TPPc							X		X	X	
NTPP											X
NTPPc										X	

TABLE III. Possible Obscuration Types for Each VRCC-3D+ Base Relation

Figure 2 shows three examples, further illustrating some of the possible combinations of the VRCC-3D+ partial overlap relation PO (as computed in 3D), and various types of obscuration (for a particular 2D projection *p*).

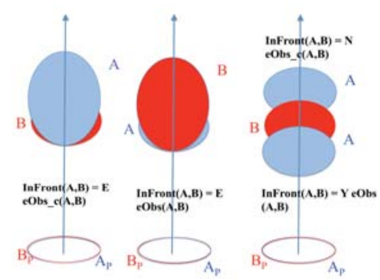

Figure 2. Examples of Partial Overlap (PO) in VRCC-3D+

C. *The Conceptual Neighborhood Graph*

As previously mentioned, a conceptual neighborhood graph (CNG) represents the possible transitions from one relation to another. Expansion of the set of relations for VRCC-3D+ necessitated the construction of a new CNG.

Table IV shows all the inter-relation distances, computed in the same manner as was discussed for the earlier model, VRCC-3D.

	DC	EC	PO	EQ	TPP	TPPc	NTPP	NTPPc
DC	0	1	4	6	5	5	4	4
EC	1	0	3	5	4	4	5	5
PO	4	3	0	6	3	3	4	4
EQ	6	5	6	0	3	3	4	4
TPP	5	4	3	3	0	6	1	7
TPPc	5	4	3	3	6	0	7	1
NTPP	4	5	4	4	1	7	0	6
NTPPc	4	5	4	4	7	1	6	0

TABLE IV. Inter-relation Distances for Base Relations

However, the calculation of intra-relation distance for VRCC-3D+ is different since it now includes the qualitative relative distance between a pair of obscuration types. An example of the computation is as follows. As displayed in Table V, since pObs is valid when IntExt is empty or non-empty, the IntExt contribution to the distance between pObs and cObs is 1 if they are different, or 0 if they are the same. In order to cover uncertainty (not knowing which occurs in actual instance), we use a distance of 0.5, the average of 0 and 1, for matching {∅, ¬∅} with {∅} or {¬∅}. For *InFront*, Y represents "closer", N represents "farther", and E ("equal") is midway between; thus, it was decided to use 1 for the difference between Y and N, and 0.5 for the difference between E and Y, or E and N. The conceptual distance for each pair of obscuration types is given in Table VI.

	IntInt	IntExt	ExtInt	InFront
pObs	¬∅	{∅,¬∅}	¬∅	Y
cObs	¬∅	¬∅	∅	Y
cObs_c	¬∅	∅	¬∅	N
nObs_e	∅	¬∅	¬∅	E

Table V. Predicates Used to Compute Intra-Relation Distance (e.g., distance between pObs and cObs is 1.5, cObs and cObs_c is 3, and cObs_c and nObs_e is 2.5)

	nObs	nObs_c	nObs_e	pObs	pObs_c	pObs_m	eObs	eObs_c	eObs_e	cObs	cObs_c
nObs	0	1	0.5	1.5	2.5	1.5	3	4	3.5	2	3
nObs_c	1	0	0.5	2.5	1.5	1.5	4	3	3.5	3	2
nObs_e	0.5	0.5	0	2	2	1	3.5	3.5	3	2.5	2.5
pObs	1.5	2.5	2	0	2	1	1.5	2.5	2	1.5	1.5
pObs_c	2.5	1.5	2	2	0	1	2.5	1.5	2	1.5	1.5
pObs_e	1.5	1.5	1	1	1	0	2.5	2.5	2	1.5	1.5
eObs	3	4	3.5	1.5	2.5	2.5	0	1	0.5	1	2
eObs_c	4	3	3.5	2.5	1.5	2.5	1	0	0.5	2	1
eObs_e	3.5	3.5	3	2	2	2	0.5	0.5	0	1.5	1.5
cObs	2	3	2.5	1.5	1.5	1.5	1	2	1.5	0	3
cObs_c	3	2	2.5	1.5	1.5	1.5	2	1	1.5	3	0

TABLE VI. Intra-Relation Distances for Obscuration Types

The row and column headings of Table VII correspond to a partial set of the VRCC-3D+ relations; the complete table is too large to display herein. The entries in the table are symmetric. Each relation is within three of the conceptual distance to its nearest neighbors. Six relations are within 0.5, eleven are within 1+0, and fifteen are within 0+1. Eight edges of length 0+1.5 and three edges of length 3+0 also were selected to yield a connected graph of conceptual neighbors for the set of VRCC-3D+ relations.

A graphic depiction of the CNG is shown in Figure 3. The nodes in the CNG are grouped vertically by their base relations, and horizontally by their possible obscuration relations. This arrangement facilitates the visual distinction between the inter-relation distance and the intra-relation distance. All edges in the graph are undirected.

It should be noted that there are different methods for constructing a CNG, and not all such methods will produce the same graph; the number of edges may vary depending upon the construction method utilized. Furthermore, depending upon the semantics of the particular set of relations being modeled, some construction methods will not produce a useful CNG. For example, the Snapshot Model approach [10] could not be utilized (without significant modifications) for VRCC-3D+. Application of that algorithm resulted in a collection of disconnected subgraphs, some of which contained nodes for relations that were more closely related based on inter-relation topological distance, while others contained nodes for relations that were more closely related based on intra-relation topological distance. As future work, other approaches for constructing the CNG will be considered and analyzed to determine any benefits over the All-Pairs-Shortest-Path (graph) approach that the authors did use.

		PO	PO	EQ	TPP	TPP	TPPc	TPPc	TPPc	NTPP	NTPPc
		pObs	eObs	eObs_e	eObs_c	eObs_e	eObs	eObs_e	cObs	cObs_c	cObs
PO	pObs	0	0+1.5	6+2	3+2.5	3+2	3+1.5	3+2	3+1.5	4+1.5	4+1.5
PO	eObs	0+1.5	0	6+0.5	3+1	3+0.5	3+0	3+1	3+1	4+2	4+1
EQ	eObs_e	6+2	6+0.5	0	3+0.5	3+0	3+0.5	3+0	3+1.5	4+1.5	4+1.5
TPP	eObs_c	3+2.5	3+1	3+0.5	0	0+0.5	6+1	6+0.5	6+2	1+1	7+2
TPP	eObs_e	3+2	3+0.5	3+0	0+0.5	0	6+0.5	6+0	6+1.5	1+1.5	7+1.5
TPPc	eObs	3+1.5	3+0	3+0.5	6+1	6+0.5	0	0+0.5	0+1	7+2	1+1
TPPc	eObs_e	3+2	3+0.5	3+0	6+0.5	6+0	0+0.5	0	0+1.5	7+1.5	1+1.5
TPPc	cObs	3+1.5	3+1	3+1.5	6+2	6+1.5	0+1	0+1.5	0	7+3	1+0
NTPP	cObs_c	4+1.5	4+2	4+1.5	1+1	1+1.5	7+2	7+1.5	7+3	0	6+3
NTPPc	cObs	4+1.5	4+1	4+1.5	7+2	7+1.5	1+1	1+1.5	1+0	6+3	0

TABLE VII. Partial Table of Minimum Distance Edges

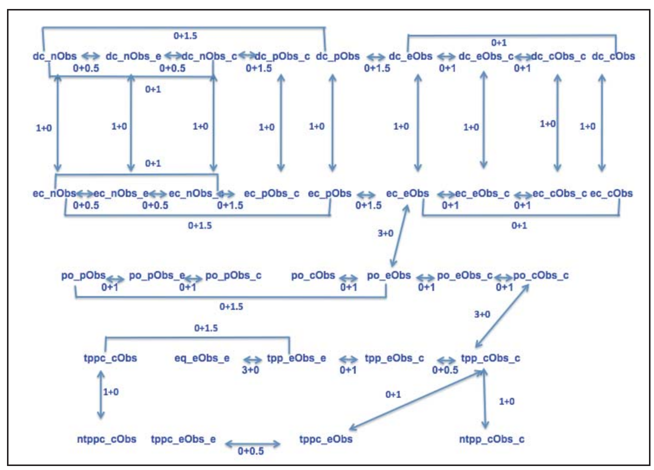

Figure 3. VRCC-3D+ Conceptual Neighborhood Graph

D. The Composition Table

Given the VRCC-3D+ relation R_1 between A and B, and the relation R_2 between B and C, we can determine R, the set of all "possible" composite (spatial and occlusion) relations for A and C. First, a composition table (CT) for only the base relations is computed, as is a CT for only the obscuration relations. These tables are then integrated based on which types of obscurations are possible for each spatial relation. Due to space limitations, the complete VRCC-3D+ composition table is not displayed here.

A simplified real-world example illustrates the potential usefulness of the CT, as well as the benefits of the more informative spatial knowledge that is considered by VRCC-3D+ (which is not present in other RCC-based models). Suppose that three airplanes, A, B, and C, of equal size are flying in the sky. If the air controller only knows that A and B are in disjoint regions, and that B and C are in disjoint regions, then the RCC-8 CT entry for A and C is universal (i.e., it could be any possible RCC-8 relation); hence, there is no guarantee that A and C cannot crash. As shown in Table VIII, even the corresponding entries in the VRCC-3D CT for this configuration cannot provide that assurance. However, additional depth information relative to the viewer, such as A is farther away from B, and B is farther away from C, is taken into consideration in VRCC-3D+. In this particular situation, the VRCC-3D+ CT entry for A and C is a single relation (i.e., A and C are disconnected, and A completely obscures C from the viewpoint of interest); thus, by consulting the VRCC-3D+ CT, we know that in the given configuration A and C will not crash.

VRCC-3D	DC_COBS(B,C)
DC_COBS(A,B)	**DC_COBS(A,C), EC_COBS(A,C), NTPPC_COBS(A,C), PO_COBS(A,C), TPPC_COBS(A,C)**
VRCC-3D+	DC_ cObs(B,C)
DC_ cObs(A,B)	**DC_cObs(A,C)**

TABLE VIII. Comparison of a Composition Table Entry for VRCC-3D and VRCC-3D+

IV. FUTURE WORK

In addition to the aforementioned investigation of additional methods for constructing the CNG, future work will include testing an implementation of the VRCC-3D+ reasoner on a variety of datasets from different domains (e.g., anatomy, mechanical design, etc.) to analyze its usefulness, accuracy, and scalability. We then plan to further enhance the model, considering additional dimensions of information such as time and physical properties (e.g., transparency, translucency, and repulsion). It is anticipated that such enhancements will require the definitions of additional predicates (similar to the *InFront* predicate discussed herein), and, more challengingly, the identification of valid combinations of all the various attributes.

V. CONCLUSIONS

In this paper we presented an extension of our previous work to combine quantitative and qualitative reasoning in 3D. The enhanced model, VRCC-3D+, is more expressive in that it now distinguishes several types of obscuration. Further, it differs from other region connection calculi in that it determines the composite relation between two objects in 3D, not just 2D. Given the greater wealth of information that can be obtained when additional dimensions are considered, and the enormous amount of 3D image data that are available, we are optimistic that this work will contribute to the implementation (and adoption) of software that more closely replicates human cognitive spatial reasoning.

VI. REFERENCES

[1] J. Albath, J. Leopold, C. Sabharwal, and A. Maglia, RCC-3D: Qualitative Spatial Reasoning in 3D, *Proceedings of the 23rd International Conference on Computer Applications in Industry and Engineering (CAINE 2010)*, Las Vegas, NV, Nov. 8-10, pp. 74-79, 2010.

[2] D.A. Randell, Z. Cui, and A.G. Cohn, A Spatial Logic Based on Regions and Connection., *KR*, 92, pp. 165–176, 1992.

[3] B. Bennett, Spatial Reasoning With Propositional Logics, *Proceedings of the 4th International Conference on Principles on Knowledge Representation and Reasoning (KR-94)*, Bonn, Germany, pp. 165-176, 1994.

[4] A.G. Cohn, B. Bennet, J. Dooday, and N.M. Gotts, Qualitative Spatial Representation and Reasoning with the Region Connection Calculus, *GeoInformatica* 1(1), pp 1-44, 1997.

[5] J.O. Yang, Q. Fu, and D. Liu, A Model for Representing Topological Relations Between Simple Concave Regions. *ICCS 2007, Part I, LNCS 4487*,Y. Shi et al., Editors, pp. 160-167, 2007.

[6] A.P. Galton, Lines of Sight, in *AISB Workshop on Spatial and Spatio-Temporal Reasoning*, 1994.

[7] D.A. Randell, M. Witkowski, and M. Shanahan, From Images to Bodies: Modelling and Exploiting Spatial Occlusion and Motion Parallax, *IJCAI-01*, pp. 57-63, 2001.

[8] J. Albath, J. Leopold, and C. Sabharwal, Visualization of Spatio-Temporal Reasoning Over 3D Images, *Proceedings of the 2010 International Workshop on Visual Languages and Computing* (in conjunction with the *16th International Conference on Distributed Multimedia Systems*), Oak Brook, IL, Oct. 14-16, 2010, pp. 277-282.

[9] M. Egenhofer and K. Al-Taha, Reasoning about Gradual Changes of Topological Relationships, *Theories and Methods of Spatio-Temporal Reasoning in Geographic Space*, A. Frank, L. Campari, and U. Formentini, Editors, Lecture Notes on Computer Science 639, pp. 196-219, 1992.

[10] M. Santos and A. Moreira, Conceptual Neighborhood Graphs for Topological Spatial Relations, *Proceedings of the 2009 World Congress on Engineering*.,Vol. I, London, UK, July 1-3, 2009.